The STM Study of Bi Adsorption on the InAs(111)B Surface

Jung-Ching Liu

Division of Synchrotron Radiation Research

Physics Department, Faculty of Science

A Master's thesis equivalent to 30 credits

Duration: 5 months

LUND UNIVERSITY

Supervisor and Co-Supervisor:

Anders Mikkelsen

Sandra Benter

Spring, 2019

Abstract

Semiconductors composed of group III and group V elements have a variety of promising applications, such as topological insulators and quantum computers. Among this category of semiconductors, bismuth (Bi)-containing III-V compounds are able to make these applications possible. However, the difficulty was found to alloy Bi atoms into the host lattice.

To solve the problem of material fabrication, we need to understand how Bi atoms affect the structure of the host material. In this thesis, we chose to study the Bi adsorption on the indium arsenide (InAs) (111)B surface. Bi atoms were evaporated from a solid source, and deposited on the InAs(111)B surface. Scanning tunneling microscopy (STM) was used to investigate the surface morphology, as well as distinguish the difference between different deposition durations and the effect of annealing.

From STM images, we found that deposited Bi atoms tend to scatter around as single atoms, and then aggregate into small islands. The growth of Bi films were prohibited due to the short diffusion length on the substrate, since the deposition was done at room temperature. In addition, we also found Bi-induced substrate reconstruction after the deposition. From deposition tests, we noticed that the Bi morphology is sensitive to experimental parameters, such as the Bi source temperature. Thus, the key to improve the reproducibility of the results is the precise control over the source temperature. After annealing the Bi-deposited substrate, the number of Bi clusters decreases significantly, meanwhile, some holes were left on the surface.

Our study is just the first step of understanding the Bi adsorption behavior. The next step will be combining the STM results with other techniques to obtain quantitative and structural information of the surface. Also, the adsorption on nanowires (NWs) is of high interests, since the large surface-to-volume ratio of NWs may exhibit highly different properties from the surface of a bulk.

Acknowledgement

First of all, I would like to thank my supervisor, Anders Mikkelsen. Thank you for giving me advice about how to do the experiment, and guiding me to write a thesis. Lacking of sufficient lab experience, my experimental plan was a bit disordered at the beginning. Thanks for pointing a way for me, and suggesting the reasonable order of doing experiments. I learned a lot of experimental skills with your guidance.

I would also like to thank my co-supervisor, Sandra Benter. You are an excellent teacher of STM. Thanks for your patience of guiding me to familiarize the STM operation, details about sample preparation, and all the things I need to know to conduct the experiment independently. I will not forget the pleasant time we had in the STM lab.

Rainer, thanks for helping me out when I met some problems in the STM lab. Also, thank you for arranging the beamtime in Aarhus. Even though the beamtime did not go smoothly, it was a valuable experience for me to learn practical knowledge of a synchrotron facility.

I would like to extend my gratitude towards all the members in the STM group. Especially Yen-Po and Yi, your help and advice always came in time.

There are also a number of nice people I met in Sweden who helped me go through the tough year of thesis work. Thank Shih-Wen (Winnie) and Jenn-Min (Jimmy) for your occasional invite to your cozy house. Delicious Taiwanese dishes, desserts, and the after dinner talk lit up my heart and helped me survive the dark winter. Junhua, thank you for spending time listening to my complaint when I was stressed out by the experimental work.

Finally, I would like to show my appreciation to my family. Without your solid support, I could not have made up my mind to pursue my Master's degree in a foreign country, and gone this far in my life.

Contents

List of Abbreviations

III-V ..... Binary compounds that are composed of one III group and one V group elements

LDOS ..... Local Density of States

LEED ..... Low-energy electron diffraction

ML ..... Monolayer

NW ..... Nanowire

STM ..... Scanning Tunneling Microscopy

UHV ..... Ultra High Vacuum

WZ ..... Wurtzite

XPS ..... X-ray photoemission spectroscopy

ZB ..... Zincblende

1 Introduction

Many properties of semiconductors lie between conductors or insulators. Take electrical conductivity for example, at room temperature, semiconductors act like insulators, however, with certain amount of applied bias, electrons can be driven in semiconductors and current flow is thus generated. A common approach to enhance the conductivity is doping elements (often III, IV, and V group elements) into the material. Taking advantage of this characteristics, semiconductors play an important role in electronics, and change our lives significantly.

One category of semiconductors is composed of III group and V group elements (III-V compounds). This type of semiconductors is of great scientific interest due to their diverse properties. Properties of III-V compounds can be easily modified by adjusting the percentage of components, or incorporating different elements into the material. In recent years, bismuth (Bi) is an element that arouses attention among scientist and engineers. As the largest atom of the V group elements, Bi is known for its strong spin-orbit coupling, which is important for topological insulators and quantum computing [1]. Furthermore, with Bi incorporation, one can expect the enhancement in spin-orbit coupling of the III-V-Bi alloy, and a large band gap reduction [2]. The band gap engineering with Bi has great potential on optical applications, and photodetectors in near- to mid-infrared range is one example among them [3].

Not only the bulk semiconductor materials, the science of their surfaces is also a field that many scientists are interested in. As the termination of the bulk material, the surface morphology may change in order to reduce the number of unfavored broken bonds. To directly observe the surface morphology, scanning tunneling microscopy (STM) is a powerful tool for the investigation. With STM, the surface topography is plotted according to the variation of tunneling current between the tip and the surface. Since the tunneling current is sensitive to the tiny difference in the distance, the height variation in the scale of a few ångströms is able to be detected. This characteristic of STM makes it a suitable technique to visualize the sample surface in atomic scale.

Although Bi-containing materials have many promising properties and applications, one of the problems is the poor ability for Bi atoms to incorporate into other III-V substrates [3]. As previously mentioned, Bi is the element that has the largest atomic size among group V elements, which may lead to the poor ability to alloy into a much smaller host III-V lattice. Before utilizing the material into applications, we should first understand the material fabrication as well as the science behind it, which is also the aim of the thesis.

In this thesis, we study the Bi adsorption behavior via STM. The indium arsenide (InAs) (111)B surface is chosen as the host material. We evaporate Bi from the solid and deposit Bi atoms on the InAs(111)B surface. The deposited morphology is then studied with STM. Based on images taken from STM as well as known adsorption theories, the Bi adsorption behavior on the InAs surfaces can be understood.

2 Theory

The study of the adsorption behavior is important in various fields. For instance, how well reactants adsorb on the catalyst surface will affect the ability of catalysis. For epitaxial crystal growth, the adsorption of incoming atoms is the first step for the process. In this chapter, general theories about adsorption at the solid-gas interface, growth mechanisms, and the surface morphology will be discussed.

2.1 Adsorption Theory

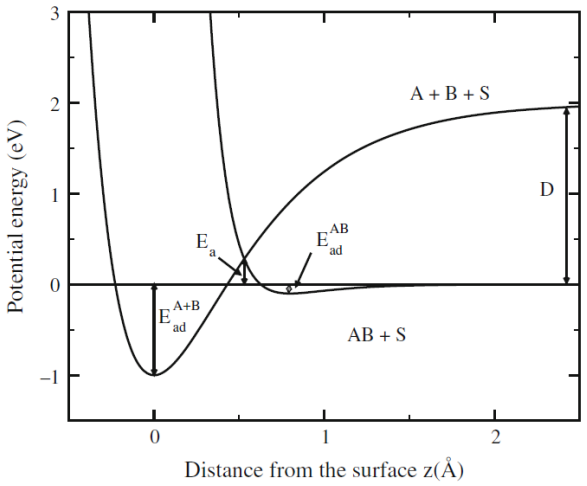

Figure 2.1: The potential energy diagram for adsorption. [4]

The adsorption behavior can be characterized by the type of interaction between adsorbates and the substrate. Adsorbates can adsorb on the substrate surface through physical (physisorption) or chemical (chemisorption) bonding. The energy diagram in figure 2.1 shows the potential energy when an adsorbate molecule is approaching the substrate. The shallow well in the diagram indicates weak bonding between the molecule AB and the substrate S. This weak interaction is known as physisorption, to which mainly contributed by van der Waals force with energy around 0.1 eV [4]. One the other hand, the other curve that has a deeper well corresponds to chemisorption. This strong interaction is the result of forming chemical bonds. In addition, as shown in the plot, much less energy is required for the molecule AB to dissociate when it is adsorbed on the surface (E_a) than as a free-standing molecule (D). This characteristic is often utilized in the catalysis process: reactants dissociates much faster if they are attaching on the catalyst surface, and the

reaction rate can thus be significantly elevated.

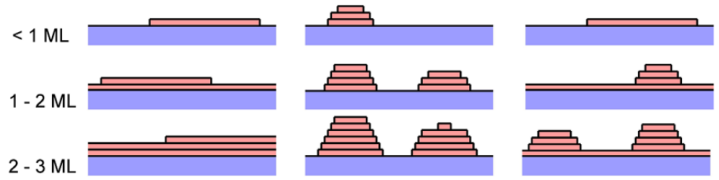

Figure 2.2: The three classical growth patterns. From the top to the bottom shows successive growth with increasing number of adsorbed monolayers (MLs). (Left) Layer growth. (Middle) Island growth. (Right) The mixture of layer and island growth. [5]

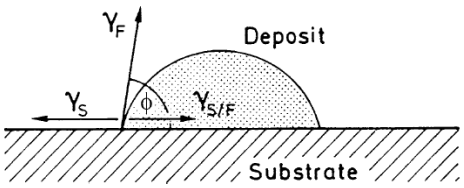

Figure 2.3: A scheme of a droplet formed by the accumulation of adatoms. [6]

Adsorption is also the foundation of crystal growth. Despite of the complexity of final crystal structures, a thermodynamically favored structure is the result of minimizing the total surface free energy. During the growth process, three common patterns can be found: layer growth, island growth, or layer-plus-island growth (figure 2.2). To predict the crystal growth pattern, one can consider a simplified scheme of a deposited droplet on a substrate as shown in figure 2.3. An important factor that involves in the growth process is the surface tension (γ), which originates from the energy required to create a new surface or interface [6]. There are three different surface tensions in the system: the surface tension of the substrate (γ_S), the surface tension of the film (γ_F), and the surface tension at the substrate/film interface ($\gamma_{S/F}$). The relationship among these surface tensions can be found by applying the equation of force equilibrium:

$$\gamma_S = \gamma_{S/F} + \gamma_F cos\phi, \tag{1}$$

with ϕ the contact angle, which depends on the bonding affinity between the deposited material and the substrate. In the qualitative perspective, a simple method to predict the growth pattern is comparing the energy before and after the presence of the newly grown

structure. The layer growth takes place when the energy for exposing the substrate is greater than the energy sum of generating the substrate/film and film/vacuum interfaces ($\gamma_S \geq \gamma_{S/F} + \gamma_F$). Besides, the layer growth is characterized by its zero contact angle, indicating good wetting on the substrate. The island growth occurs when the relation is the opposite: $\gamma_S < \gamma_{S/F} + \gamma_F$. This means that larger energy is needed to generate new interfaces than maintain the clean substrate surface. Island growth also comes with poor bonding affinity between the two materials, which lead to $\phi > 0$.

The cause for the mixture of layers and islands is different from simply considering the strength of the bonds. In a hetero-growth environment, due to the lattice mismatch between the deposited layer and the substrate material, strain accumulates as the film becomes thicker. After reaching a certain thickness, island growth dominates in order to relax the strain in the films [5, 6].

For predicting crystal growth, surface tension is just a rough estimation. In the practical growth process, we also need to take kinetic factors, such as desorption and diffusion, into account.

2.2 Surface Structure

Instead of simply being the termination of a solid, surfaces have their distinctive structures and properties compared with the bulk. Due to the broken bonds created by cutting the solid, the configuration of the topmost atomic layer tends to change significantly to reduce the large amount of energy on the surface. Two of the common rearrangements are relaxation and reconstruction. As shown in figure 2.4, relaxation is the case when the spacing between the top two layers differs from the periodic atomic spacing in the bulk. On the other hand, reconstruction is a more violent way of atom rearrangement. Broken bonds can be reduced by forming bonds with neighboring atoms or missing a whole row, leading to a configuration that is different from the ideal structure of the corresponding plane.

Because of highly oriented covalent bonds in semiconductors, the semiconductor surface generally exhibits a much more severe reconstruction comparing with the metal surface,

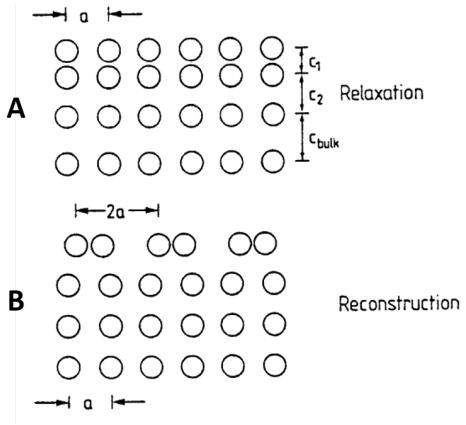

Figure 2.4: A scheme of the side view for relaxation and reconstruction of the surface. Assuming a cubic crystal with lattice constant a: (A) for relaxation, the spacing of top layers is smaller than the normal lattice spacing of the bulk (c_{bulk}); (B) for reconstruction, the lateral periodicity of the surface layer is different from that of the bulk. [6]

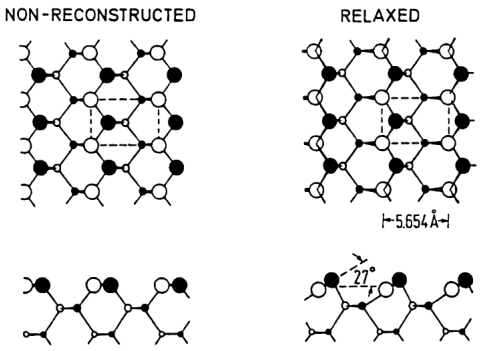

Figure 2.5: A schematic view of ideal and relaxed GaAs(110) surface. Black circles are As atoms, white circles are Ga, and smaller ones are atoms at deeper layers. (Upper) Top view, the (1×1) unit cell is marked by dashed rectangle. (Lower) Side view. [6]

which is built with non-oriented metallic bonds. At a semiconductor surface, neighboring dangling bonds at the top layer tend to form chemical bonds with one another. This process can largely reduce the number of unsaturated bonds created at a newly cut surface. For III-V compounds, due to the different numbers of valence electrons between these two kinds of elements, further stabilization can be fulfilled by tilting bonds [5–7]. Figure 2.5 is a GaAs(110) surface which shows the result of the reconstruction process mentioned above. In the left penal, the ideal Ga-As bond is parallel to the bulk, while in the real surface, the Ga-As bond relaxes and As atoms tilt upwards with the angle around 27° as the right panel shows [6]. This reconstruction process can further stabilize the structure. Aside from the tilting the bonds at the top most layer, some other planes exhibit more

complicated reconstruction, such as the GaAs(100) surface. It is possible for a GaAs(100) plane to have multiple reconstructed structures that depend on the temperature and other growth parameters. The surface investigated in this project is the InAs(111)B surface. The structure of the InAs(111)B surface will be discussed in chapter 3.2.1, and the STM observation will be shown in chapter 4.1.

3 Experimental Method

In this thesis project, we investigated Bi deposition on the InAs(111)B substrate via scanning tunneling microscopy (STM). The theory and the operation principles of STM, as well as the method for preparing samples will be discussed in this chapter.

3.1 Scanning Tunneling Microscopy

STM is a powerful tool which is able to visualize the sample surface with atomic scale resolution. The history of STM can be traced back to 1982, when G. Binnig and H. Rohrer proposed the concept of surface investigation by measuring the tunneling current between the sample and the probe with a thin vacuum layer as the tunneling barrier [8]. The STM we used has a preparation chamber and an analysis chamber. Both of the chambers are ultra high vacuum (UHV) environment in order to prevent the sample surface from oxidizing and ensure the stability of the surface morphology. In the preparation chamber, samples are cleaned and deposited with Bi. Without these preparation processes, the chamber pressure is generally maintained around 10^{-9} mbar. As for the analysis chamber, where the sample is probed, the pressure is further lowered to the scale of 10^{-10} mbar. To introduce a new sample from ambient pressure into the STM through load lock, it takes some time for the pump to lower the pressure of the load lock before being able to transfer. This time-consuming process is one drawback that limits the number of experiments that can be done.

To make the surface investigation possible, the probing device in the analysis chamber is composed of several important components: the tip, feedback system, piezo drive, and vibration damping system. First of all, a sharp tip is the basic requirement for high spatial resolution. Among all materials, tungsten (W) is widely used as the tip material due to its hardness. With a hard tip, we can secure the completeness of the tip after the accidental crash into the sample. In addition to the sharpness, the tip should also be made stiff to prevent oscillating while scanning. The tip used in our experiment is made by electrochemically etched W wire with a diameter of 0.38 mm. To nicely resolve the surface, conductivity is the principal requirement for the sample since tunneling current is the physical quantity that a STM measures. High concentration of electrons at the surface

can guarantee enough tunneling current with the tip, and thus metals or semiconductors are ideal samples for STM investigation.

During STM operation, the feedback system is crucial for adjusting the tip position. The tip adjustment includes the coarse movement to approach the tip to the sample, and the fine-tuning during the surface investigation. Both of the tip movements are done with the piezo drive. The dimension of a piezo material can be changed by applying a voltage. To utilize this property in the STM, several pieces of the piezo material are attached to the tip. By applying unequal amount of voltage to each piezo piece, the difference in the dimensional change causes the tip to bend accordingly. The piezo drive is especially useful for the fine-tuning of the tip height for the constant current mode. As the name suggests, the constant current mode keeps the tunneling current constant during scanning, and adjusts tip-sample distance to match the current setpoint. After receiving the signal from the feedback system, the piezo drive changes the tip-sample distance. Another common mode of STM is the constant height mode. In this mode, the feedback loop is turned off, and the height of the tip is thus fixed. The surface topography is plotted by recording the variation of the tunneling current.

Since the spacing between the tip and the sample is within 1 nm, tiny vibration of the system will reflect on the image. To isolate the system from any external vibration, the STM is fixed on a stiff ground, with the scanning stage suspended with springs. Further vibration damping can be done by eddy current, which is able to cancel out the out-of-balance movement of the scanning stage. Still, the internal electronic noise generated from the cords is hard to eliminate. Although it is easy to be distinguished from the image by its small and regular pattern, some surface configurations may be covered and unable to be resolved.

3.1.1 Theory

The tunneling current for STM simulation can be calculated with Tersoff-Hamann theory, which is proposed by J. Tersoff and D. R. Hamann in 1985 based on first-order perturbation theory [9]:

$$I = \frac{2\pi e}{\hbar} \sum_{\mu,\nu} f(E_\mu)[1 - f(E_\mu + eV)]|M_{\mu\nu}|^2 \delta(E_\mu - E_\nu), \tag{2}$$

where the function f is the Fermi function; V the bias voltage; E the energy of the state without tunneling; $M_{\mu\nu}$ is the element of the tunneling matrix; the index μ indicates parameters of the probe, and the index ν refers to the parameters related to the sample. The assumptions of small bias and ideal tip are made to simplify the equation. An ideal tip means that the tip apex is a point, and probes the sample with spherical s-shaped wavefunction. With these assumptions, the tunneling current in equation 2 becomes proportional to the integration of the surface local density of state (LDOS) between Fermi level (E_F) and the elevated level with bias ($E_F + eV$) at the tip position $\vec{r}$ [9]:

$$I \propto \rho_t \int_{E_F}^{E_F+eV} \rho_s(\vec{r}, E_F + \varepsilon) d\varepsilon \ , \tag{3}$$

where ρ_t is the LDOS of the tip apex, and ρ_s is the LDOS of the sample. The result above reflects directly on STM images, which means that these images can be considered as contour of surface LDOS. Although equation 3 gives a simplified conclusion to the tunneling current calculation, the assumptions have some contradiction to the real case. For example, the valance shell of a tungsten tip is the highly oriented d-orbital. Also, the small bias assumption is only suitable for metallic samples. In our project, a relatively large bias is needed to generate a tunneling window for electrons to transfer from the semiconductor sample to the tip.

3.1.2 Bias-Affected Imaging

As indicated in the equation 3, one parameter that affects the STM image is the bias voltage. The bias voltage applied on either the sample or the tip can create a Fermi level difference, causing the tunneling current to change accordingly. This technique is especially useful when investigating III-V components, since the density of filled states and empty states of the two elements are different. As figure 3.1 shows, by applying positive bias to the sample, the Fermi level is lowered with respect to that of the tip, allowing electrons to tunnel from the tip to the sample. On the other hand, if the applied bias is negative, the Fermi level of the sample is elevated, electrons tend to tunnel from the sample to the tip. Figure 3.2 [10] is an example that demonstrates the GaAs(110) surface with both positive and negative bias. As previously discussed, with positive bias,

the empty states of the sample can be plotted and Ga atoms appear to be bright, while As atoms are clearly seen for the case of negative bias, since V group elements have more filled states than III group elements.

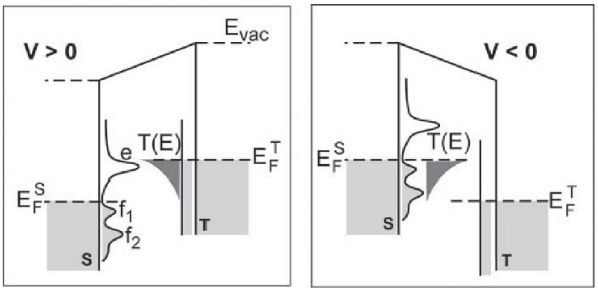

Figure 3.1: The Fermi level changes according to the direction of the bais. S stands for the sample and T stands for the tip. [11]

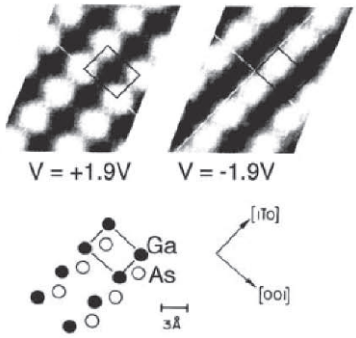

Figure 3.2: STM images of GaAs(110). The top two images show the effect induced by the positive and negative bias with the same value of 1.9 V. The lower scheme indicates the structure of GaAs(110). [10]

3.1.3 Limitations and Experimental Challenges

Although STM is a useful method for studying surface science, there are still some limitation or challenges for this technique. The image obtained from STM only shows the apparent height of the surface, which corresponds to the movement of the tip recorded by the system. The apparent height does not always represent the real topography of the sample surface. As shown in Tersoff-Hamann theory, the tunneling current is highly dependent on the LDOS, which can differ greatly among atoms and chemical environment.

Since the tunneling current depends on the density of states of both the tip apex and the sample surface, images obtained by STM can be considered as the convolution of the surface topography and the shape of the tip. During scanning, it is possible that the tip picks up some particles and becomes blunt or forms multiple sharp apexes. A step edge is a nice reference to test the sharpness of the tip. With a blunt tip, originally sharp edges become round in the height profile. In addition, a blunt tip is unable to resolve detailed structures of the surface, and loses the strength of this surface investigation technique. In the case of multiple tips, it can be recognized from an unreasonable repetitive pattern appearing. Figure 3.3 is the STM image of the clean InAs(111)B surface. In the image, pairs of triangular defects appear repetitively, with the smaller defect locates at the upper right of the larger one. Sometimes it is possible that defects appear in pairs, however, the possibility is rather low if the same pattern repeats in the whole image.

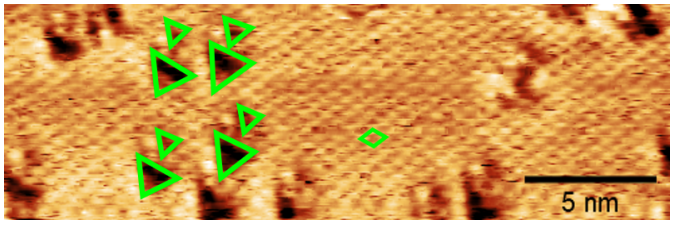

Figure 3.3: The STM image of a clean InAs(111)B surface. As indicated with green triangles, there is a repetitive pattern that a small defect locates at the upper right of the larger defect. In this image, atomic resolution is achieved. The unit cell of the InAs(111)B surface is marked by the diamond. I= 130 pA, V= -2.5 V.

Although the shape of the tip changes during scanning, there are some useful methods to reshape the tip. First, scanning on a gold film is a common approach. As an inert metal, the surface of the gold film can maintain free of oxides for a long period of time in the STM chamber. Furthermore, gold is an excellent conductor that is able to generate large tunneling current, and thus it is easy to obtain a stable STM image of the surface. With these properties, we can use a gold film to check the shape of the tip, and also reshape the tip by moderately dipping it into the film. By dipping and pulling up the tip, it is possible that the unwanted particles detach from the tip, which makes the tip become sharp again. In addition to scanning on gold, another common method to condition the tip is to apply a large voltage pulse. Adhered particles may drop off from the tip due to the pulse.

However, some limitations of this technique are difficult to overcome. In our experiment, since the surface investigation is done under room temperature, thermal vibration from the lattice may make atomic rows be observed more commonly than individual atoms. Nevertheless, signals of atomic rows sometimes can be covered by the noise generated from electronics or cables. On STM images, the pattern of noise and atomic rows are similar: both of them have regular row pattern. One method to distinguish noise from atomic rows is to change the scanning speed. With high scanning speed, the width of rows generated by noise becomes wider, and vice versa. Even though we can tell these two patterns apart, noise is still unwanted since atomic rows are unable to be seen with the presence of noise, which often has roughly the same or larger height than that of atomic rows.

What worth noticing is that the STM only probes the surface density of state, which can refer to the surface topography. However, we cannot discern element difference from a STM image. Even though we can distinguish elements of a III-V compound by tuning between positive/negative bias as previously discussed, to confirm the composition of a more complicated sample, other investigation methods are needed. Nevertheless, the high sensitivity of the local electron density of state makes STM outstand from investigation techniques such as X-ray photoemission spectroscopy or absorption spectroscopy, which only measure averaged bonding characteristics of the sample.

3.2 Sample Preparation

3.2.1 Substrate Material

Zinblende (ZB) and wurtzite (WZ) (see figure 3.4) are common crystal structures for III-V binary compounds. Atomic layers are close-packed along $\langle 111 \rangle$ for ZB crystals and $\langle 0001 \rangle$ for WZ crystals with two different stacking sequences. For a ZB crystal, atomic layers stack by repeating the order ABCABC. On the other hand, for a WZ crystal, the type of staking is composed of two alternating symmetries ABAB.

The InAs(111)B surface is the material we used to study Bi adsorption behavior. With the ZB structure, the ideal thickness of 1 ML of the (111) plane can be calculated as $a/\sqrt{3}$, where a is the lattice constant of the InAs crystal, of 6.06 Å. We can find that

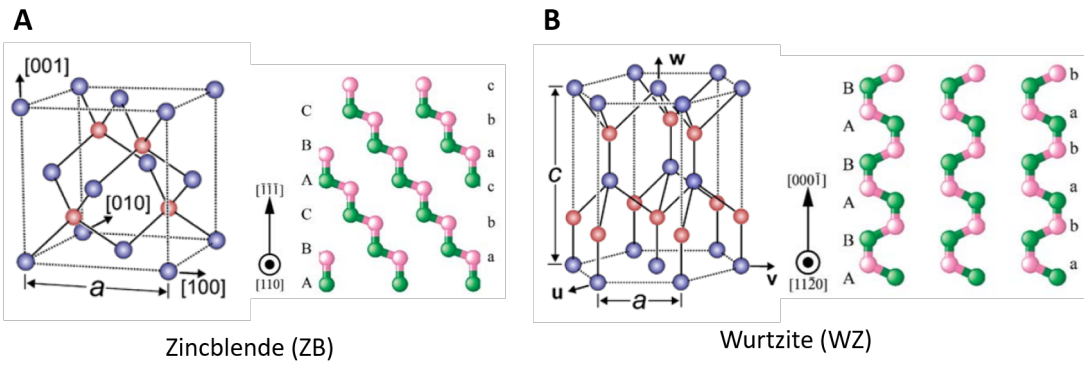

Figure 3.4: The crystal structure and the stacking sequence along the indicated direction for (A) a zincblende crystal and (B) a wurtzite crystal. Spheres with two different colors represent III and V group elements respectively. [5, 12]

1 ML thickness of InAs(111) is roughly 3.5 Å. Due to the periodicity of the crystal, the cleaved (111) plane can be terminated with both In and As atoms. The plane that has In atoms at the top most layer is the (111)A surface, and (111)B surface terminates with As atoms. For a (111)B surface, the vacancy model can be used to describe As trimers observed under STM, see figure 3.5 [13,14]. According to this model, one of every four As atoms tends to leave the surface, causing the remaining As atoms to form the triangular symmetry. As the result, the size of a unit cell is extended to (2×2).

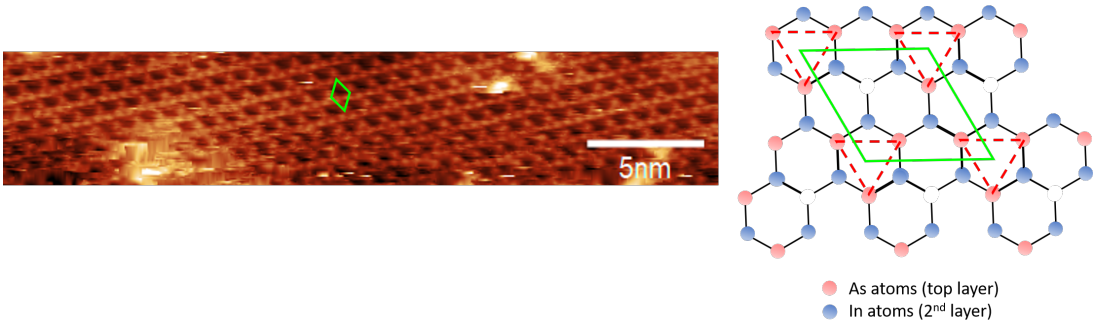

Figure 3.5: The image at the left is taken after annealing the surface in UHV after Bi deposition (I= 120 pA, V= -2.5 V). The As-trimer configuration can be explained by the As-vacancy model, which is drawn at the right. The reconstruction leads to the extension of the unit cell to the size (2×2) as indicated with the green diamond. The plot of the vacancy model is adapted from [14].

3.2.2 Cleaning Process

In our experiment, the InAs(111)B substrate is prepared by cutting a sulfur-doped n-type InAs(111)B wafer, then gluing it with In wire on a sample plate that is preheated to 200°C. Wafers taken out from the ambient environment are usually oxidized. To obtain a clean substrate, atomic hydrogen bombardment is an efficient approach to remove oxides from the sample surface. Figure 3.6 shows the scheme of a hydrogen cracker, which is commonly used for the hydrogen cleaning process. A tungsten tube is heated up by the filament to 1700°C. Meanwhile, the cooling water is circulating through the cracker to prevent the whole device from being heated up. Then the hydrogen gas is leaked into the tube, adsorbs on the wall, and leaves the tube as highly active ions. It is found that with chamber pressure around 2×10^{-6} mbar, these highly active hydrogen ions are able to effectively react with oxides on the sample surface, and those contaminants can be carried away thereafter. What worth noticing is that during hydrogen cleaning, the substrate should be heated to 380-420°C at the same time. By elevating the temperature, the substrate is annealed while cleaning, and oxides are able to possess more energy to react with hydrogen ions.

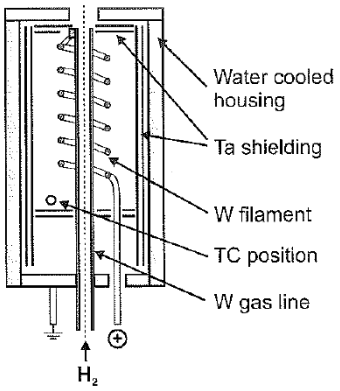

Figure 3.6: The inner structure of a hydrogen cracker. [15]

However, this cleaning process sometimes causes unwanted configuration or contamination on the surface. During a long and high temperature annealing, As atoms at the topmost layer tend to evaporate and leave triangular defects, and In atoms may form droplets on the surface. A possible contamination of this process comes from the tungsten tube of the hydrogen cracker, which may drop some particles onto the sample. Both types of contamination can be misleading when distinguishing between impurities from deposited Bi.

3.2.3 Bismuth Deposition

The Bi evaporator was newly mounted to the STM before the project started. In addition to study the adsorption behavior of Bi, testing the new evaporator becomes the secondary purpose of the project. Figure 3.7 is the scheme of the evaporator. Solid Bi is placed in a metal crucible, with heating filament wrapped around. Since the Bi source transforms from solid to liquid phase during heating, the source should be anchored at a low position (see figure 3.8). Although Bi atoms evaporate and adsorb on the sample surface with an angle, this should not affect the experiment much due to the larger opening of the evaporator over the area of the sample.

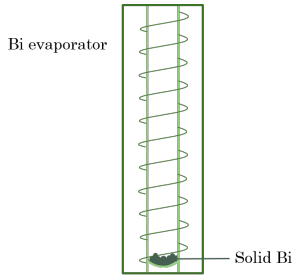

Figure 3.7: The scheme of the inner structure of the Bi evaporator used in our project.

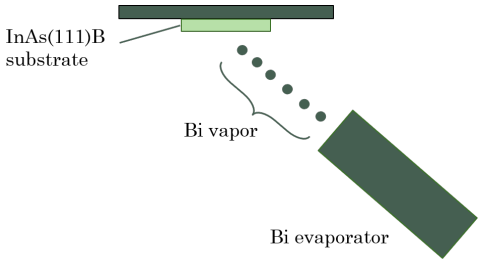

Figure 3.8: Positions of the Bi source and the substrate during deposition. The source is placed at a low position and Bi vapor impinges the substrate with an angle.

The parameters for Bi deposition are based on the previous work done by Knutsson in the University of California at Santa Barbara [12]. In Knutsson's experiment, the Bi source is heated up to 420°C, and the evaporated Bi atoms are deposited for roughly 360 seconds onto the GaAs nanowire with sample temperature at 250°C. In our project, the InAs substrate is used instead of GaAs nanowires. Since InAs is sensitive to high temperature, the substrate remains at room temperature during the deposition.

In the deposition test, it is important to have precise control over the source temperature, since the amount of evaporated Bi is sensitive to the temperature change. However, this is difficult to achieve due to the setup of the equipment. The thermocouple that measures the source temperature is not attached directly to the crucible. Thus the temperature measured may not be representative to that of the Bi source. Another uncertainty of the source temperature comes from the power supply. Overheating sometimes happens during heating up the source, which means that the speed for increasing the current of the power supply is larger than the heating speed of the filament. Since the current of the power supply is higher than the current needed to reach a certain temperature, overheating can cause gradual temperature increase during the deposition process. The inevitable measurement error from the thermocouple and overheating are reasons that may lead to the poor reproducibility of our experiment. The deposition morphology and further discussion will be mentioned in section 4.2.

4 Result and Discussion

4.1 Clean Surface

We first scanned the clean InAs(111)B surface as the comparison for the later deposition and annealing tests. Figure 4.1 is an overview of the clean surface. From the image, the edges of large stages have the triangular shape due to the symmetry of the lattice that was previously mentioned in section 3.2.1. As shown in the profile, the height of the stage is ranges between 0.3 to 0.4 nm, which fits the ideal 1 ML thickness of the (111) plane (3.5 Å). On both the top most island and the one down below, there are triangular defects in various sizes. Since the InAs(111)B substrate is heated up to the temperature range 380-420°C, some As atoms are able to possess enough energy and then evaporate from the lattice. As the result, triangular holes are left on the surface. In addition to hole defects, some protrusions can also be observed in the figure. These protrusions could be In droplets, which are also the result of annealing during the cleaning process. Another possible cause for protrusions is that they could be contaminants dropped by the tip while scanning.

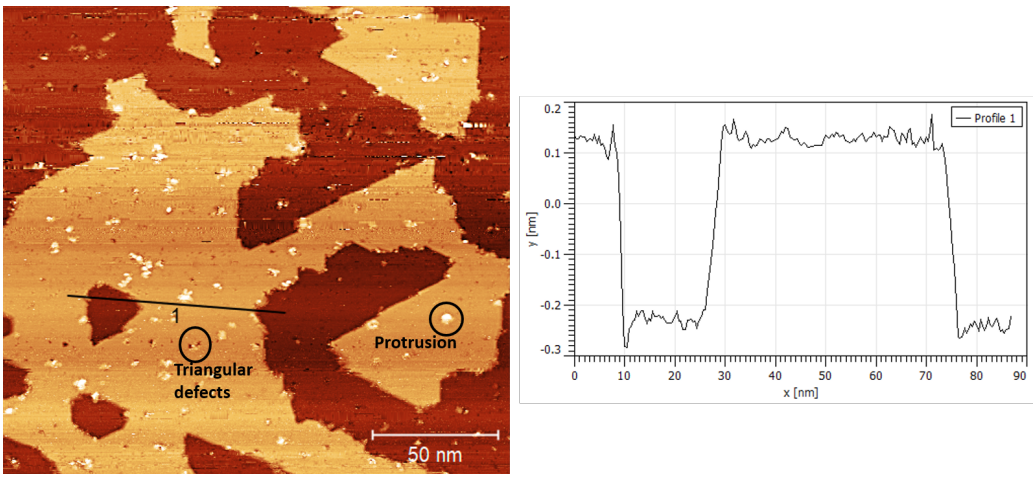

Figure 4.1: (Left) The STM image of the clean InAs(111)B surface with size 200×184.8 nm^2. I= 100 pA, V= -3 V. Examples of triangular defects and a protrusion are marked by circles. (Right) The height profile along the line indicated in the image.

Figure 4.2 shows the clean surface on a much smaller scale. In this image, although the surface pattern is elongated due to drifting, triangular defects can still be clearly seen. The size of defects in this image correspond to the missing of one As atom. These triangular defects are randomly distributed, yet pointing at the same direction. The triangular

shape comes from the hexagonal symmetry of the (111)B surface. Since our InAs(111)B substrate is cut from a single crystal wafer, these triangular defects should point at the same direction. If the substrate is multi-crystalline, the identical orientation indicates that these defects are located on the surface of the same grain, where InAs crystallizes in the identical direction. In the height profile, triangular holes are marked by red arrows. The depth of single As vacancies is around 0.2 to 0.3 nm, which is slightly smaller than the height of the stage. This result further confirms that these holes are generated by missing As atoms at the top most layer.

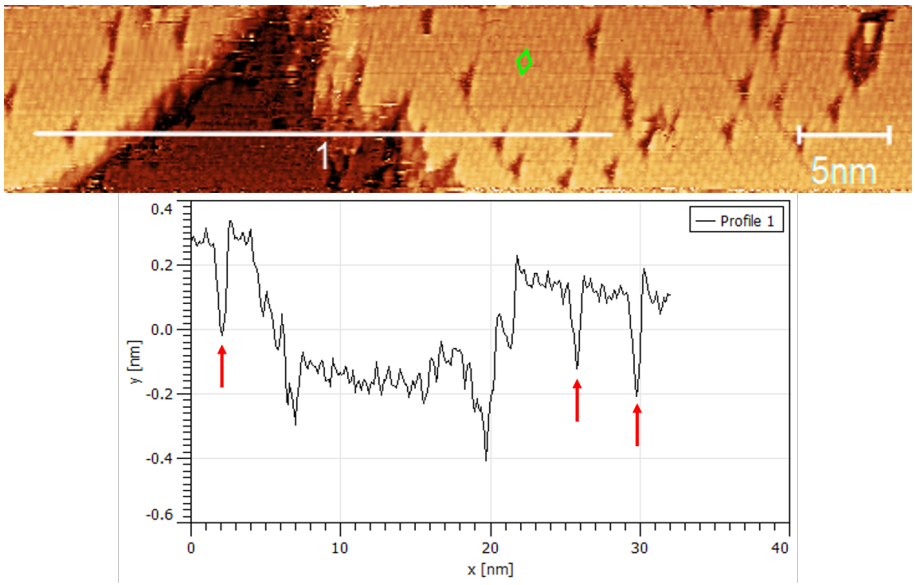

Figure 4.2: (Top) The STM image of the clean InAs(111)B surface with size 50×10 nm^2. The (2×2) unit cell is marked by the green diamond. I= 140 pA, V= -3 V. (Bottom) The height profile along the line indicated in the image. Three triangular defects crossed by the line are marked by red arrows. The depth of the defect is around 0.2-0.3 nm.

Defects are crucial for materials used in electronics. When electrons encounter defects such as vacancies or interstitial particles, they tend to scatter away and reduce the conductivity of the material. As a common index, defect density can be used as a reference of the quality of the surface. To determine the defect density, since the contrast of tiny defects in our image is not clear enough for the software to count, manual counting is an alternative. When counting defects, three areas (figure 4.3B-D) are selected from figure 4.3A based on the tip condition. Among these chosen regions, defects are classified by their sizes: tiny defects with one pixel, which can be considered as one atomic vacancy, and those that are larger than one pixel.

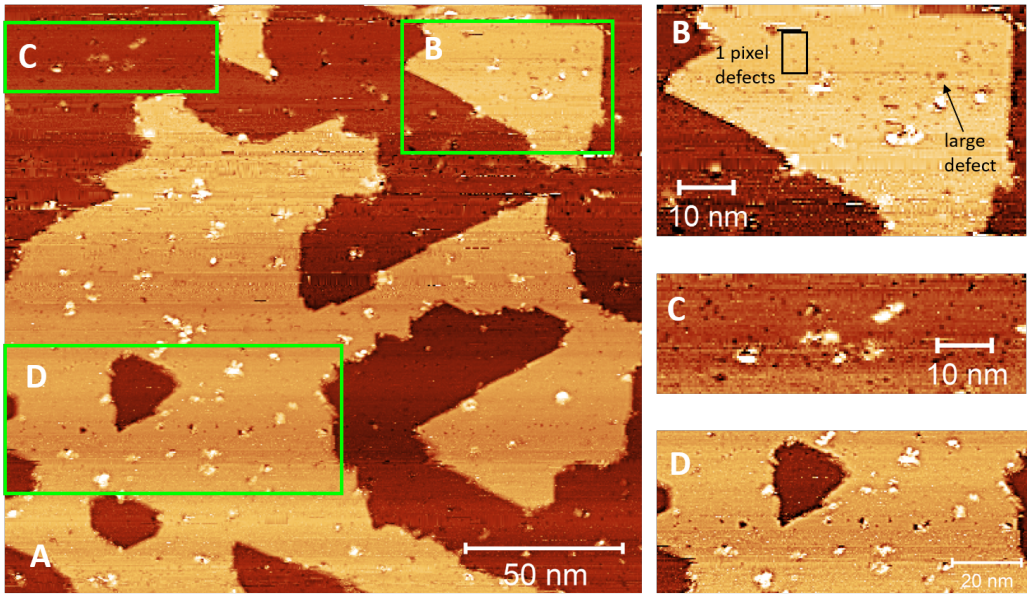

Figure 4.3: (A) The STM image of the clean InAs(111)B surface with size 200×184.8 nm^2. Triangular defects in various sizes and protrusions can be seen in the image. I= 100 pA, V= -3 V. (B) A selected area in (A) with size 66×41.2 nm^2. (C) A selected area in (A) with size 66.4×21.6 nm^2. (D) A selected area in (A) with size 105.6×46.4 nm^2.

Through counting defects in these three chosen regions, it is found that the average density of one pixel defects is $(23.38\pm0.89)\times10^{-3}$ nm^{-2}, and the density for larger defects is $(3.65\pm0.36)\times10^{-3}$ nm^{-2}. According to the result, the total number of defects in figure 4.3A can be calculated by multiplying the defect density by the area: the number of one pixel defects is 864.12±32.89, and the number of larger defects is 134.90±13.31. The manual defect counting inevitably has large uncertainty due to the change in the tip condition. In figure 4.3A, the tip becomes unstable in some regions, which may not be able to show the presence of tiny defects. Even though the three analyzed areas are chosen from the stable regions, the uncertainty can also come from the resolution of the image. Since figure 4.3A shows a rather larger field of view, defects with small sizes may be not clear enough to be counted.

Although hydrogen cleaning is able to remove oxides from the surface, with increasing number of cleaning cycles, it is possible to cause deterioration of the surface by forming more vacancies and droplets. Nevertheless, it is difficult to avoid the presence of defects on the surface.

In addition to the cleaning process, triangular defects can also be observed under other conditions according to previous studies. For instance, in the experiment done by Hilner *et al.* [16], triangular defects appeared on the InAs(111)B surface after annealing the InAs(111)B surface at 600°C in the As atmosphere in UHV. They proposed that the defect is formed as the result of the absence of one In atom, which leads to either the relaxation or desorption of the surrounding As atoms. Even though there are many possible explanation for the formation of defects, the triangular shape is usually seen due to the symmetry of the lattice.

4.2 Bismuth Deposition

After investigating the clean surface, we deposited Bi on the InAs(111)B surface to study the adsorption behavior of Bi. During the deposition, the Bi source temperature was raised to 400°C, without heating the substrate. We chose the deposition time to be 5 minutes and 10 minutes, and used two sequential 5 minutes deposition as the examination of the reproducibility.

4.2.1 Surface After 5 Minutes of Deposition

For the first part of the experiment, the InAs(111)B surface after 5 minutes of Bi deposition is examined with STM. The deposition process was done without heating the InAs(111)B substrate, which indicates that there is almost no diffusion nor incorporation of Bi atoms on the surface. Therefore, the equal probability of adsorption along edges and on terraces is expected. However, in figure 4.4, Bi clusters reside more densely along edges than on terraces.

Next, we analyze the dimension of a cluster. The number of Bi atoms in a cluster can be estimated by dividing the volume of a cluster to the volume of a Bi atom. As shown in the profile in figure 4.4, the diameter of a cluster is roughly 6.6 nm, and the height is 0.37 nm. With the assumption that the cluster has a cylindrical shape, its volume is calculated as 12.66 nm^3. The volume of a Bi atom can be approximated by the metallic Bi crystal. The unit cell of a Bi crystal has the volume around 212.46 $Å^3$ with 6 atoms. The volume of one Bi atom is roughly 35.41×10^{-3} nm^3. As the result, there are around 357 Bi atoms in this cluster.

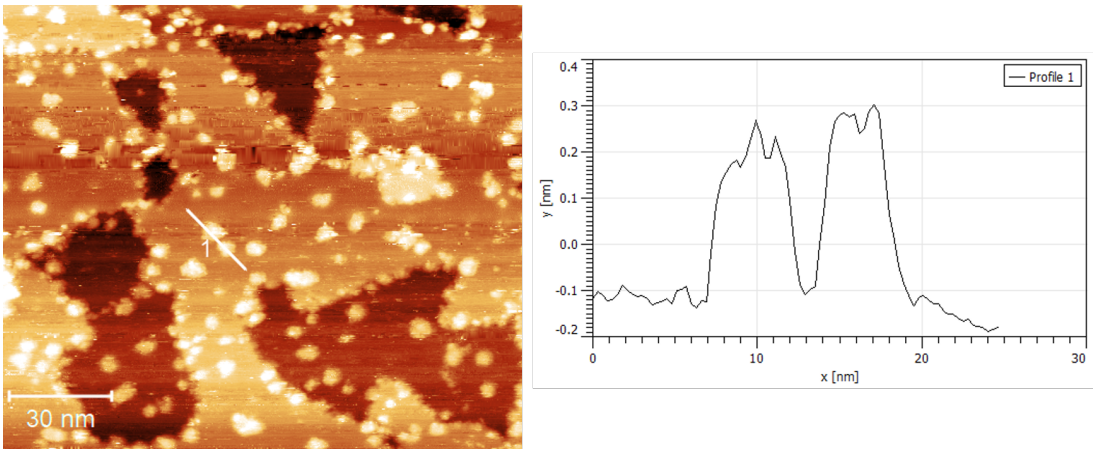

Figure 4.4: (Right) The InAs(111)B surface after 5 minutes of Bi deposition with size 150×128 nm^2. The substrate was maintained at room temperature, and the Bi source was heated to 406°C and increased to 415°C due to overheating. The chamber pressure was 8×10^{-9} mbar during the deposition. I= 100 pA, V= -2.8 V. (Left) The height profile along the indicated line in the STM image.

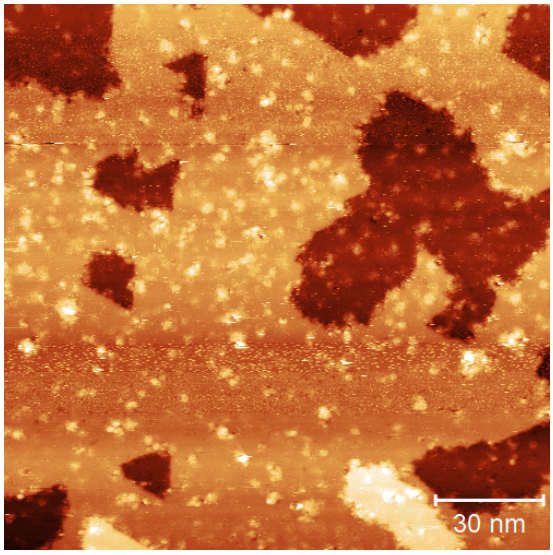

Figure 4.5: The result of another 5 minutes Bi deposition test. The InAs(111)B substrates was maintained at room temperature. The source temperature raised from 399 to 403°C, with chamber pressure 5×10^{-9} mbar during the deposition. The image size is 150×150 nm^2. I= 140 pA, V= -3 V.

Figure 4.5 shows a separate 5 minutes deposition experiment. These two images are taken with the identical magnification under STM, but the size, shape, and distribution of Bi clusters are different. This can be the result of imprecise control over the Bi source temperature. Due to overheating, the source temperature exceeds the target temperature (400°C) during the deposition. As the consequence, the temperature range (406-415°C for figure 4.4, and 399-403°C for figure 4.5) and the Bi vapor pressure (8×10^{-9} mbar for figure 4.4, and 5×10^{-9} for figure 4.5) differ from each experiment. To improve the stability of the source temperature, we need to avoid overheating and start depositing only when the source temperature stays stable. This, however, can be time-consuming and thus limits the repetition of experiment that can be done.

In addition, in figure 4.5, the tendency for Bi clusters to reside along edges is not as clear as in figure 4.4. Since these two images are taken from two separate samples, except for different deposition parameters discussed above, different defect densities of the two clean surfaces may also generate distinct deposited morphology. Different defect densities are the results of the difference in parameters during each substrate cleaning process, such as the hydrogen pressure, substrate temperature, or the substrate annealing time. With these defect sites, either protrusions or triangular holes, on clean terraces, Bi atoms are possible to change their adsorption behavior, and distribute more evenly on the surface, instead of residing densely along edges. Likewise, the surface morphology for the following deposition and annealing experiments can also be affected by the quality of the clean substrate. This is also the reason that makes the clean surface investigation important.

4.2.2 Surface After 10 Minutes of Deposition

In the next deposition test, we extended the deposition duration to 10 minutes. An overview of the surface is shown in 4.6. From the image, Bi clusters distribute evenly, and form a number of small islands with irregular shapes. Since the Bi source was heated above the melting point (271°C), the deposited Bi atoms still have some mobility even without annealing the substrate. The mobility is yet limited, and only the short distance of diffusion is allowed. Therefore, it is difficult for small islands to grow, and large islands are not seen in this image. This observation also indicates that Bi atoms do not tend to form films on the InAs(111)B surface, which requires a long diffusion length, if the

substrate is not annealed.

However, this observation can be related to many parameters, such as the Bi vapor pressure and the deposition duration. With a higher Bi vapor pressure or a longer deposition time, more Bi atoms will occupy on the surface, which leads to hindrance of the diffusion and less positions left to choose from. As the result, incoming Bi atoms reside at unfavored sites. The surface morphology may be no longer the same with different experimental parameters.

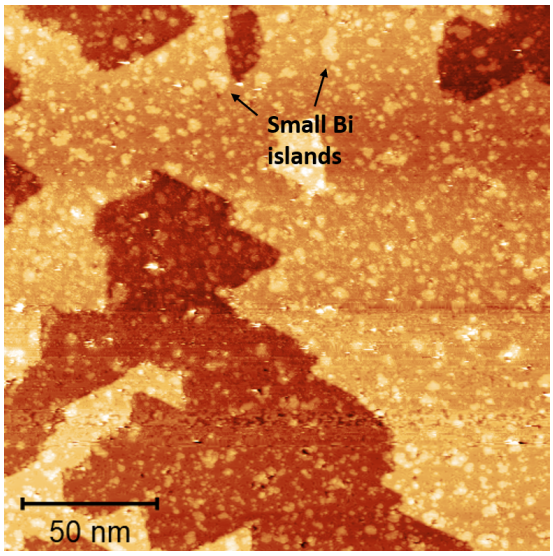

Figure 4.6: The InAs(111)B surface after 10 minutes of Bi deposition with size 200×200 nm^2. The substrate was maintained at room temperature, and the Bi source was heated to 395°C and increased to 421°C when the deposition ended. The chamber pressure was 6×10^{-9} mbar during the deposition. I= 100 pA, V= -3 V.

With the large magnification (see figure 4.7A), clusters and curves on the substrate are clearly seen. There are two very different morphologies of clusters: individual round clusters and aggregations of them. Profile 1 in figure 4.7 plots the height variation of two individual round clusters. From the profile, the height of each cluster is around 0.2 nm, and the width is 1.7 nm. The height roughly fits the size of a Bi atom, which has the radius of 0.14 nm [17]. Thus, these round "clusters" are actually individual Bi atoms. Comparing the width with that measured for 5 minutes deposition (figure 4.4 with height 0.37 nm and width 6.6 nm), we found that there is a large difference in the width. As mentioned in section 3.1.3, the STM image can be considered as the convolution of the

tip shape and the surface topography. The combined effect of different magnification and tip condition is the convincing reason that individual Bi atoms are unable to be seen in figure 4.4.

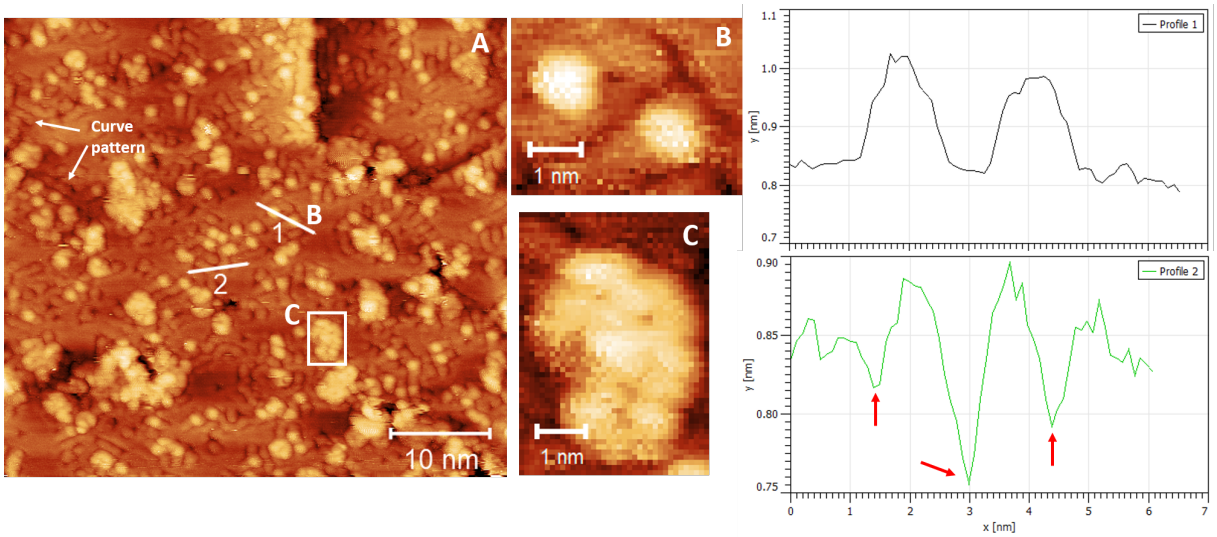

Figure 4.7: (A) A zoom-in of the InAs(111)B surface after 10 minutes of Bi deposition with size 50×45.6 nm^2. Individual Bi atoms as well as their aggregations are randomly distributed on the surface. There are also some curve patterns on the substrate, which can be induced by deposited Bi. (B) Shows two round Bi atoms crossed by line 1 in (A). Image size: 4.3×3.3 nm^2. (C) The aggregation of Bi atoms marked in (A). Image size: 3.7×5.1 nm^2. I= 120 pA, V= -2.8 V. Profile 1 and 2 plot the height variation of single Bi atoms and the curve pattern respectively. In profile 2, positions of ditch-like curves are marked by red arrows.

By comparing the size, a single cluster in the 5 minutes deposition test corresponds to an aggregation of Bi atoms in the 10 minutes test. Based on the results above, we can find the evolution of Bi clusters on the InAs(111)B surface. The deposited Bi atoms (figure 4.7B) tends to aggregate as clusters (figure 4.7C), and then grow into small islands.

In addition to clusters, curve patterns are also observed on the substrate after 10 minutes of deposition. A possible cause for the curve pattern is Bi-induced reconstruction of the substrate surface. These curves do not follow a specific order, and they appear at the vicinity of Bi atoms or clusters. From profile 2 in figure 4.7, the depth of the curve is roughly 30 to 40 pm, and the deeper one is around 80 pm. All of these values are much

smaller than the depth of a triangular hole (0.2-0.3 nm) as discussed in section 4.1. The shallow depth indicates that these curves only occur near the surface, and no atoms are missing in the curves. Moreover, profile 2 also shows that the substrate protrudes slightly outward between two curves comparing with that without the curve pattern. This further points out the reconstruction of the substrate: atoms at the top most layer move closer to each other, and the dense packing leads to the slight protrusion with ditch-like curves left at their original positions.

4.2.3 Surface After Two Sequential 5 Minutes of Deposition

To test the reproducibility of our experiment, we deposited additional Bi for 5 minutes after the first 5 minute deposition. From figure 4.8, in addition to Bi clusters with irregular shapes, these reconstruction curves are similar pattern to that in figure 4.7A. This result shows nice consistency with the 10 minutes deposition. Nevertheless, there are still some difference in the density of Bi clusters. Bi clusters after the second 5 minutes deposition distribute less densely comparing with the surface after 10 minutes deposition (figure 4.6). This means that two sequential deposition is a more gentle approach for depositing Bi.

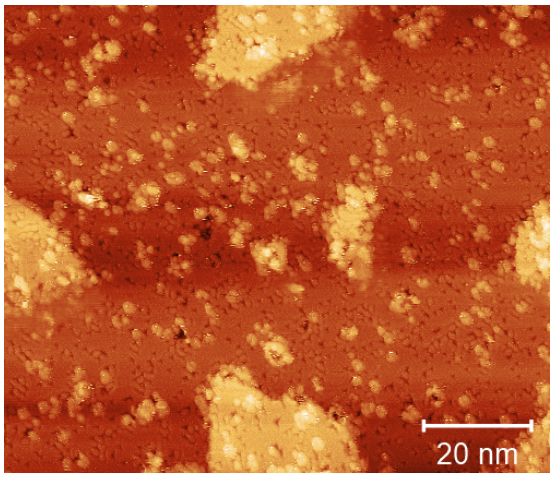

Figure 4.8: The STM image after the second 5 minutes Bi deposition. The Bi pressure for the second deposition is 4×10^{-9} mbar, with source temperature 399-420°C. The curve pattern is found to be similar to that after 10 minutes deposition, yet Bi clusters distribute less densely than its counterpart. The image size is 100×85.8 nm^2. I= 140 pA, V= -2.6 V.

In all the deposition experiments, we met the problem of overheating the Bi source. The longer deposition duration means a much larger temperature range during the deposition. For instance, 9 degrees for 5 minutes deposition, and 26 degrees for 10 minutes deposition. Since the similar pattern was seen after two sequential 5 minutes deposition, dividing the long deposition duration into several short periods could be an applicable method to improve the stability of the Bi source temperature.

4.3 Annealing

Since the Bi deposition was done without annealing the InAs(111)B substrate, the deposited Bi is considered to be randomly distributed. Through annealing the substrate after deposition, Bi atoms are able to possess enough energy to diffuse to their favored positions, escape from the surface, or incorporate into the lattice.

The samples deposited with Bi were annealed for 10 minutes at 300°C, which is slightly higher than the melting point of Bi (271°C). A large number of Bi clusters formed after 10 minutes deposition (figure 4.9A) disappear after annealing (figure 4.9B). By heating up the substrate, the loosely bound Bi atoms are able to possess enough energy and leave the surface.

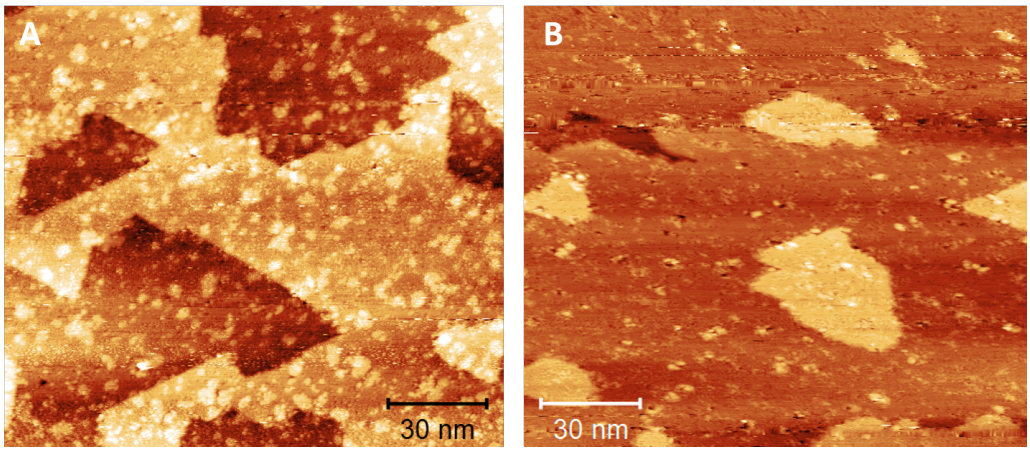

Figure 4.9: (A) The surface after 10 minutes of Bi deposition, with Bi source temperature 395-421°C. Image size: 150×132.6 nm^2. I= 100 pA, V= -2.8 V. (B) The same surface as (A), taken after being annealed for 10 minutes at 298-308°C. The slight distortion of the image is caused by the drifting of the tip. Image size: 150×131.7 nm^2. I= 100 pA, V= -2.8 V.

Figure 4.10 shows the same surface as figure 4.9B with large magnification. In the figure, there are some remaining Bi atoms, large holes and those that are much smaller. Profile 1 in the figure shows the consistency of the dimension of Bi atoms as observed in deposition tests. The depth of a large hole is shown in profile 2, which is around 0.4 nm. The value of the depth indicates that the large hole is a triangular defect of the InAs(111)B surface. These defects are either existing since the clean surface, or generated by losing As atoms due to the annealing process. There are also some holes with smaller sizes. As profile 3 shows, the depth of a small hole is around 0.1 nm. This value falls between the depth of reconstructed curves and triangular holes. These tiny holes may be the remaining reconstructed structure induced by Bi atoms. Unlike the Bi-induced reconstruction observed in deposition tests, these holes scatter around on the substrate, instead of appearing only at the vicinity of Bi atoms/clusters. This means that the Bi deposition is possible to change the underlying substrate structure, and the reconstruction remains after our annealing process.

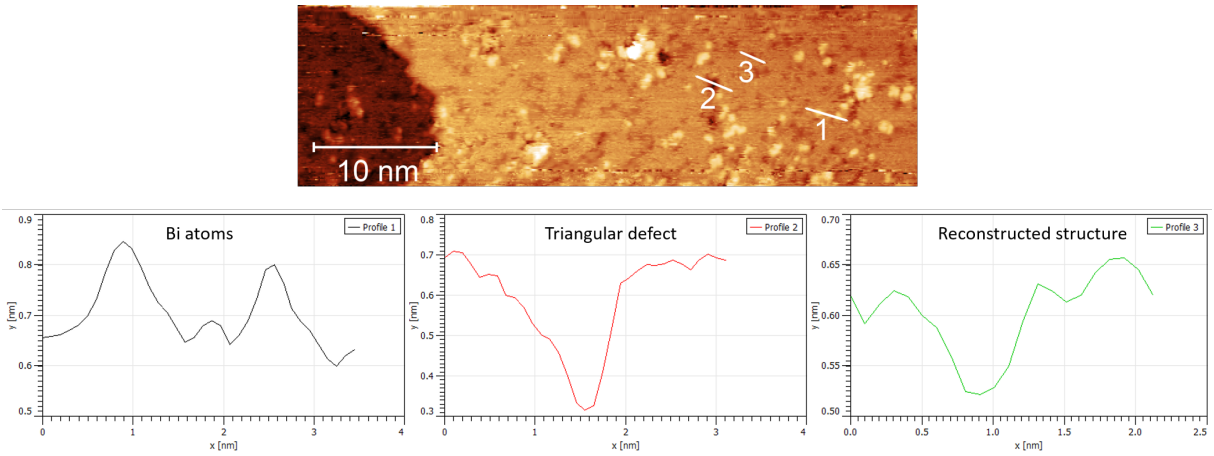

Figure 4.10: The image that shows the surface after 10 minutes of annealing with large magnification. The height variation of Bi atoms, a triangular defect, and the reconstructed structure are plotted in profile 1, 2, and 3 respectively. Image size: 50×14.6 nm^2. I= 130 pA, V= -3 V.

From deposition and annealing experiments, we found that the result is determined by kinetics. For instance, different speeds for increasing the Bi source temperature cause different degrees of overheating. As the consequence, the amount of evaporated Bi and thus the deposited morphology are no longer the same. Other parameters, such as the

annealing temperature, or the heating rate during annealing are all possible factors that can influence the surface morphology. This also makes each experiment unique. To further confirm our observation and proposed explanation, we need more repetitions and parameter adjustment.

5 Conclusion

For the purpose of studying Bi adsorption behavior on the InAs(111)B surface, we heated the Bi source to around 400°C and deposited Bi atoms onto the surface, and STM was used to investigate the surface morphology. The STM images we obtained clearly show distinct surface morphology with respect to different experimental parameters.

Before the deposition test, we probed the clean InAs(111)B surface as the reference for the later experiments. It is found that there are already some defects, either triangular holes or protrusions, on the surface. Triangular holes are the result of losing As atoms as the substrate was annealed during the cleaning process. As for protrusions, they can be In droplets which also escape from the lattice.

The Bi deposition was done with three different deposition duration: 5 minutes, 10 minutes, and two sequential 5 minutes deposition. With the substrate remains at room temperature, we observed both single Bi atoms as well as Bi clusters adsorbing on the surface. Some of the Bi clusters can even grow to 12.66 nm^3. At room temperature, Bi atoms do not tend to form large islands or films due to the limited diffusing ability on the substrate. In addition to Bi clusters, from the result of 10 minutes deposition and two sequential 5 minutes deposition, we also found the curve pattern on the substrate. Since these curves are shallow in depth, we supposed they are the result of Bi-induced reconstruction.

During the deposition test, overheating often occurred when heating up the Bi source, and the unstable source temperature may affect the deposited morphology. However, it is difficult to fix the source temperature during the whole deposition duration. An alternative is to slowly heat the source, and start depositing after the temperature becomes stable around the target temperature. Another method is to deposit Bi in a short period time, since the range of overheating becomes larger as the deposition duration increases. The applicability was confirmed from our results of 10 minutes and two sequential 5 minutes deposition.

After the 10 minutes deposition, the sample was annealed at around 300°C for 10 minutes. Bi atoms were evaporated from the surface, leading to a significant decrease in the number of Bi clusters. From the image, there are several tiny holes on the substrate, whose depth does not fit a triangular defect nor the Bi-induced curve. Still, we supposed they are the remaining reconstructed structure of the InAs even though Bi atoms are evaporated from the surface. This hypothesis can be further verified by using other investigation techniques to see if the subtract crystal structure changes.

During the deposition tests, in order to obtain the same surface morphology, it is crucial to have the identical process with the same parameters. To have better reproducibility of surface morphology, we need to precisely control the Bi source temperature, deposition time, heating and cooling rate during annealing, just to name a few.

6 Outlook

Although STM is a strong tool for probing the surface morphology, to understand the adsorption behavior of Bi in the whole scope, we need the combination with other investigating techniques. For instance, to distinguish the type of bonding and chemical composition on the surface, X-ray photoemission spectroscopy (XPS) is a suitable option. We can also learn quantitative information from a XPS spectrum, such as the coverage of Bi on the surface. Another technique that often collaborates with STM is low-energy electron diffraction (LEED). With a thick layer of deposited Bi, it is possible that Bi crystallizes on the surface, and LEED is capable of visualizing the crystal structure with diffraction patterns.

After studying the Bi adsorption on the InAs(111)B surface, the next substrate for the deposition experiment would be the InAs nanowires (NWs). The deposition on NWs is considered to have great value for scientific research. Since a NW has multiple side facets, the deposited morphology could be very different among these facets. In addition, the crystal structure of a NW can be fabricated into mixed sections of WZ and ZB, which enables the comparison of Bi adsorption between these two structures. Furthermore, a NW has a large surface-to-bulk ratio due to its rod shape, which means that many of the properties may be different from the surface of a bulk material. The research of depositing Bi atoms on a NW can serve as the fundamental for broadening the application of semiconductors.

The surface characterization of Bi on the InAs(111)B surface is just the starting point in the field of modifying material properties. There are many works left for the future, such as quantitative analysis, and deposition on NWs. Nonetheless, modifying semiconductor properties, or band structure engineering are undoubtedly promising fields of research. We expect that the research field can grow intensively and change our lives in the near future.

References

[1] H. Huang, J. Liu, and W. Duan. Nontrivial Z_2 topology in bismuth-based III-V compounds. *Physical Review B*, 90:195105–1–195105–6, 2014.

[2] M. P. Polak, P. Scharoch, and R. Kudrawiec. First-principles calculations of bismuth induced changes in the band structure of dilute Ga-V-Bi and In-V-Bi alloys: chemical trends versus experimental data. *Semiconductor Science and Technology*, 30:1–9, 2015.

[3] L. Wang, L. Zhang, L. Yue, D. Liang, X. Chen, Y. Li, P. Lu, J. Shao, and S. Wang. Novel Dilute Bismide, Epitaxy, Physical Properties and Device Application. *Crystals*, 7(63):2–62, 2017.

[4] Axel Groß. *Adsorption on Surfaces*, pages 101–163. Springer Berlin Heidelberg, Berlin, Heidelberg, 2009.

[5] Udo W. Pohl. *Atomistic Aspects of Epitaxial Layer-Growth*. Springer Berlin Heidelberg, Berlin, Heidelberg, 2013.

[6] Hans Lüth. *Morphology and Structure of Surfaces, Interfaces and Thin Films*, pages 65–127. Springer International Publishing, Cham, 2015.

[7] Pekka Laukkanen and Marko Punkkinen. *Unusual Bi-Containing Surface Layers of III-V Compound Semiconductors*, pages 225–261. Springer New York, New York, NY, 2013.

[8] G. Binning and H. Rohrer. Scanning Tunneling Microscopy. *Surface Science*, 126:236–244, 1983.

[9] J. Tersoff and D. R. Hamann. Theory of the scanning tunneling microscope. *Physical Review B*, 31(2):805–813, 1985.

[10] R. M. Feenstra, Joseph A. Stroscio, J. Tersoff, and A. P. Fein. Atom-Selective Imaging of the GaAs(110) Surface. *Physical Review Letters*, 58(12):1192–1195, 1987.

[11] Peter Sutter. *Scanning Tunneling Microscopy in Surface Science*, pages 969–1024. Springer New York, New York, NY, 2007.

[12] Johan Valentin Knutsson. *Atomic Scale Characterization of III-V Nanowire Surfaces*. PhD thesis, Lund University, 2017.

[13] A. Taguchi. First-principles investigations of surface reconstructions of an InAs(111)B surface. *Journal of Crystal Growth*, 278:468–472, 2005.

[14] A. Taguchi and K. Kanisawa. Stable reconstruction and adsorbates of InAs(1 1 1)A surface. *Applied Surface Science*, 2528:5263–5266, 2006.

[15] Dr. Ebrl MBE-Komponenten GmbH, Josef-Beyerle-Str. 18/1 71263 Weil der Stadt Germany. *Hydrogen Atomic Beam Source*, 2018.

[16] E. Hilner, E. Lundgren, and A. Mikkelsen. Surface structure and morphology of InAs(111)B with/without gold nanoparticles annealed under arsenic or atomic hydrogen flux. *Surface Science*, 604:354–360, 2010.

[17] E. Clementi, D. L. Raimondi, and W. P. Reinhardt. Atomic Screening Constants from SCF Functions. II. Atoms with 37 to 86 Electrons. *The Journal of Chemical Physics*, 47(4):1300–1307, 1967.